Ventricular Zone Gene-1 (vzg-1) Encodes a Lysophosphatidic Acid Receptor Expressed in Neurogenic Regions of the Developing Cerebral Cortex

Jonathan H. Hecht,*‖ Joshua A. Weiner,‡‖ Steven R. Post,‖ and Jerold Chun§‖

*Department of Biology, ‡Neurosciences Graduate Program §Member, Neurosciences and Biomedical Sciences Graduate Program, ‖The Department of Pharmacology, School of Medicine, University of California, San Diego, La Jolla, California 92093-0636

Abstract. Neocortical neuroblast cell lines were used to clone G-protein–coupled receptor (GPCR) genes to study signaling mechanisms regulating cortical neurogenesis. One putative GPCR gene displayed an in situ expression pattern enriched in cortical neurogenic regions and was therefore named *ventricular zone gene-1* (*vzg-1*). The *vzg-1* cDNA hybridized to a 3.8-kb mRNA transcript and encoded a protein with a predicted molecular mass of 41–42 kD, confirmed by Western blot analysis. To assess its function, *vzg-1* was over-expressed in a cell line from which it was cloned, inducing serum-dependent "cell rounding." Lysophosphatidic acid (LPA), a bioactive lipid present in high concentrations in serum, reproduced the effect seen with serum alone. Morphological responses to other related phospholipids or to thrombin, another agent that induces cell rounding through a GPCR, were not observed in *vzg-1* overexpressing cells. *Vzg-1* overexpression decreased the EC_{50} of both cell rounding and G_i activation in response to LPA. Pertussis toxin treatment inhibited *vzg-1*–dependent LPA-mediated G_i activation, but had no effect on cell rounding. Membrane binding studies indicated that *vzg-1* overexpression increased specific LPA binding. These analyses identify the *vzg-1* gene product as a receptor for LPA, suggesting the operation of LPA signaling mechanisms in cortical neurogenesis. Vzg-1 therefore provides a link between extracellular LPA and the activation of LPA-mediated signaling pathways through a single receptor and will allow new investigations into LPA signaling both in neural and nonneural systems.

A CRITICAL event in the formation of the mammalian cerebral cortex is the ordered generation of its neurons from a discrete proliferative region overlying the cerebral ventricles, the ventricular zone (vz)[1] (6), (Fig. 1). In most mammalian species, neurogenesis occurs during fetal life when the vz can be delineated by histological stains, or by brief pulses of 5-Bromo-2′-deoxyuridine (BrdU) or [³H]thymidine, which identify neuroblasts undergoing S-phase (58, 64, 67). Cortical neuroblasts display a stereotyped change in their morphology that is linked to their proliferation. During S-phase of the cell cycle, vz neuroblasts appear bipolar, with the cell body at the super-

ficial margin of the vz and with processes oriented towards the ventricular and superficial (pial) surfaces of the cerebral wall. With the progression of the cell cycle, the neuroblast undergoes "interkinetic nuclear migration" whereby its nucleus descends to the ventricular surface during G2, its pial process is retracted, and the cell "rounds up" (62, 63). After rounding, the cell undergoes mitosis and then regains its bipolar morphology to complete the cell cycle (Fig. 1 *a*). In the mouse, cortical neurogenesis is limited to the period between embryonic day 11 (E11) and E18 (9, 10, 67). Beyond this period, cells are still produced within the cerebral wall; however, these cells are generally of glial rather than neuronal lineages (4, 10, 22, 32, 67).

The molecular mechanisms responsible for controlling vz neurogenesis are largely unknown. However, three observations suggest that it is regulated, at least in part, by interactions between a neuroblast and its environment, rather than through cell-autonomous mechanisms. First, a number of growth factors operating through receptor tyrosine kinases (RTKs) (3, 78), most notably basic fibroblast growth factor, promote proliferation of telencephalic cells in primary culture (8, 30, 44, 70). Second, uncharacterized serum factors appear to be required in addition to

1. *Abbreviations used in this paper:* aa, amino acid; BrdU, 5-Bromo-2′-deoxyuridine; CNS, central nervous system; E, embryonic day; GPCR, G-protein–coupled receptor; LPA, lysophosphatidic acid; LPC, lysophosphatidylcholine; LPE, lysophosphatidylethanolamine; LPG, lysophosphatidylglycerol; PA, phosphatidic acid; PTX, pertussis toxin; RT, room temperature; RTK, receptor tyrosine kinase; TM, transmembrane; vz, ventricular zone; *vzg-1, ventricular zone gene-1.*
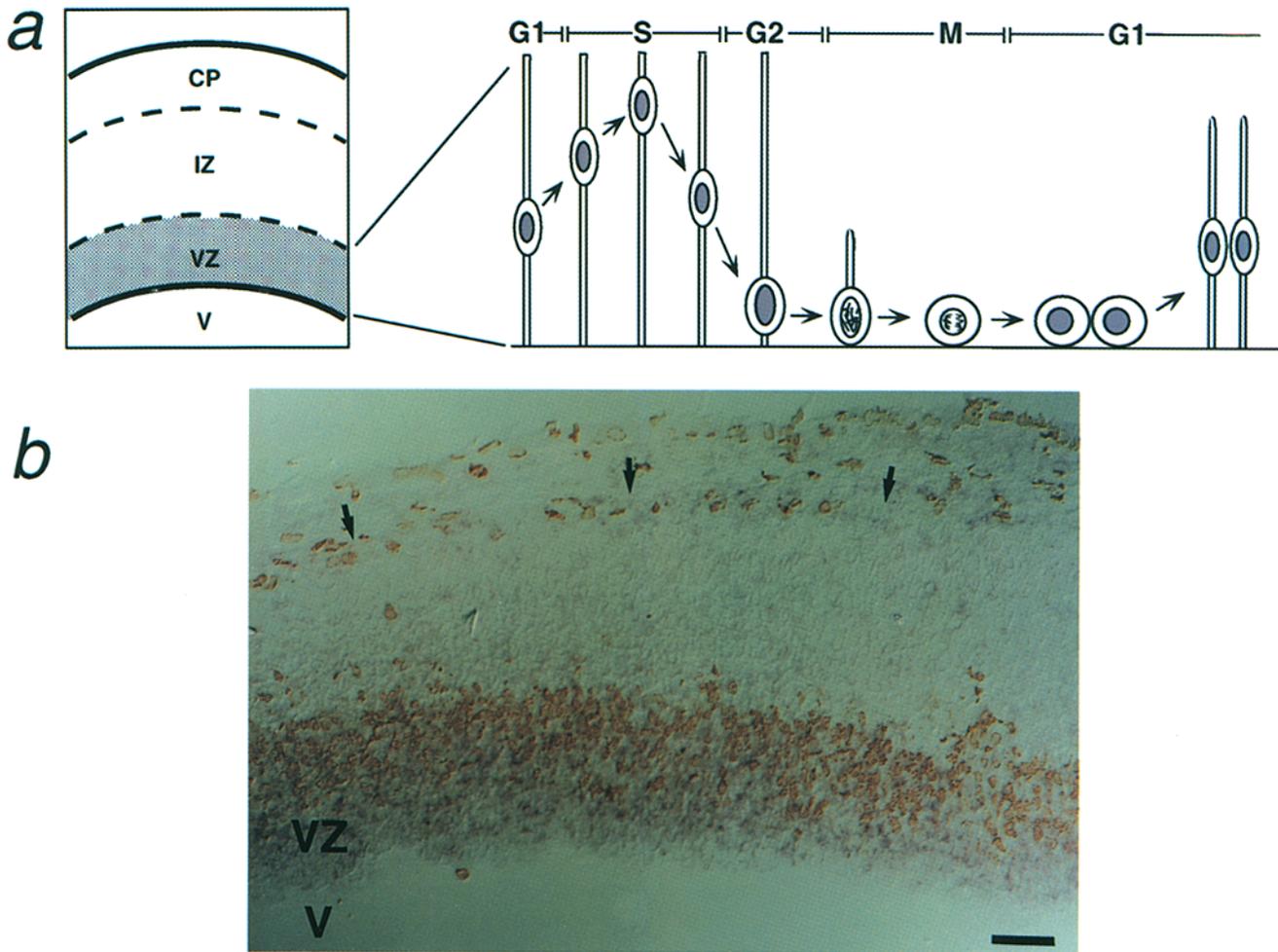
Figure 1. Location and morphologies of mitotic cortical neuroblasts within the vz. (*a*) The left diagram illustrates the anatomical zones in the embryonic cerebral cortex. Cortical neurogenesis is restricted to the proliferative vz (*shaded*). The right diagram shows the changes in proliferating neuroblast morphology during progression of the cell cycle within the vz. During S phase, cell nuclei are in the outer portion of the vz and then assume a rounded appearance closely apposed to the ventricle (*V*) by M phase. After mitosis, rounded daughter cells regain their bipolar morphology. *V*, ventricle; *VZ*, ventricular zone; *IZ*, intermediate zone; *CP*, cortical plate. (*b*) *Vzg-1* mRNA colocalizes with cortical neuroblast proliferation. Cortical neuroblasts were labeled with a 1-h pulse of BrdU (brown reaction product) to identify cells undergoing DNA synthesis (58, 68). *Vzg-1* expression was localized in the same section by in situ hybridization of an antisense digoxigenin-labeled *vzg-1* riboprobe visualized by immunohistochemistry (*purple reaction product*). Note that *vzg-1* expression is limited to the proliferative zone defined by BrdU labeling. Arrows delineate upper limit of the CNS. Bar, 50 μm.

identified growth factors to promote cortical cell proliferation (43, 44), consistent with normal cortical development in mice with null mutations for known growth factors and/or their receptors (45). Third, cell membranes or cell–cell contacts also promote proliferation of telencephalic blasts (30, 69). These observations could be explained by the operation of novel receptors, distinct from RTKs, regulating cortical neurogenesis.

An attractive candidate for this role is the G-protein–coupled-receptor (GPCR) family. It is crucial to central nervous system (CNS) function (20) and contains many diverse members (7, 57), some of which have known mitogenic effects (1, 41, 74). To isolate GPCR genes, we used novel clonal cell lines derived from the vz that resemble cortical neuroblasts (14). These cell lines provide a unique source of cDNA for cloning strategies and can further be used for functional studies of receptor genes, enabling an

identified receptor to interact with signaling pathways approximating those found in vivo.

Here we report the complete sequence and developmental CNS expression pattern of a new member of the GPCR family named *ventricular zone gene-1* (*vzg-1*) because of its restricted expression within the cerebral cortical vz (Fig. 1 *b*). Based on functional assays, ligand binding data, and its tissue distribution, we conclude that *vzg-1* encodes a receptor for lysophosphatidic acid (LPA). LPA is a phospholipid signaling molecule that has a wide variety of effects on many different cell types (see Discussion; for recent reviews see 26 and 54). Although LPA almost certainly acts through a GPCR, a cDNA clone of this receptor has not been identified, in part reflecting the chemical characteristics of LPA that result in unacceptably high levels of nonspecific binding, making techniques such as expression cloning impractical. Therefore, the possibility

that nonreceptor mechanisms could account for observed effects of LPA has been left open (26, 71, 74, 77). To overcome these difficulties, we have instead relied on well-defined functional characteristics of LPA signal transduction to identify the *vzg-1* gene product as a receptor for LPA.

Materials and Methods

Cell Culture

Cell lines TSM and TR (14) were grown in OptiMEM I (GIBCO BRL, Gaithersburg, MD) with 5% FCS (Hyclone Labs, Logan, UT), 20 mM glucose, 55 μM 2-mercaptoethanol, 100 U/ml penicillin, and 100 μg/ml streptomycin at 37°C, 5% CO_2.

Cell Transfection. Transient transfection used calcium phosphate precipitation (12) with a 10:1 molar ratio of *vzg-1* expression plasmid to β-galactosidase expression plasmid pCMVβ (Clonetech, Palo Alto, CA). After 18 h, cells were refed, grown for 24 h, fixed in 4% paraformaldehyde in PBS for 10 min, and stained for β-galactosidase activity (2). Positive cells (200/plate) were counted "blind." The statistical program Instat (Graphpad Software, San Diego, CA) was used for one-way analysis of variance and the Student-Newman-Keuls pairwise *t*-test. Stable transfection used a 10:1 molar ratio of *vzg-1* expression plasmid to pSV2-puro (79) and selection in medium containing 10 μg/ml puromycin. After 2 wks of selection, single colonies of cells were picked using cloning cylinders, expanded, and then stored or processed for RNA isolation and Northern analyses as previously described (14, 19).

Morphological Assay. Stable cell lines (5,000/well in 24-well plates) were serum starved for 24 h, and then media containing the desired agents was added to the required final concentration. Cells were fixed in 4% paraformaldehyde in PBS to terminate incubation and examined. Experiments were performed in duplicate (200 cells counted/well) and representative samples were evaluated by multiple investigators. Statistical methods used were identical to transient experiments.

cAMP Assay. Cells (30,000) were plated, serum starved overnight, and then stimulated for 7 min at 37°C with serum-free medium containing 200 μM 3-isobutyl-1-methylxanthine, 10 μM isoproterenol, and LPA. cAMP accumulation was measured as described (55). Data were analyzed using Prism (Graphpad Software).

Pertussis Toxin (PTX) Treatment. Cells were treated with 200 ng/ml PTX for 16 h, followed by a 3-h treatment with fresh PTX.

Molecular Biological Techniques

PCR Amplification of GPCR Family Members. Poly-A+ RNA was isolated from TR and TSM cells (twice selected on oligo-dT cellulose [Pharmacia LKB Biotechnology, Piscataway, NJ]) (2) and 10.5 μg of RNA was reverse transcribed using oligo-dT or random hexamer primers in 50 mM Tris, pH 8.3, 6 mM MgCl$_2$, 40 mM KCl, 1 mM DTT, 1 mM each dNTPs, and 10 U/μl Moloney murine leukemia virus reverse transcriptase (GIBCO BRL). RNA and primers were heated to 65°C (5 min), then cooled to room temperature (RT). Additional reagents were added, and then heated to 37°C (2 h). This cDNA was PCR amplified using a degenerate primer set derived from the conserved regions of transmembrane (TM) domain II and VII of the GPCR family (7). PCR reactions used 40 ng of cDNA in 10 mM Tris, pH 8.3, 50 mM KCl, 2 μM of each primer, 1.5 mM MgCl$_2$, 0.2 μM each dNTPs, and 2.5 U Taq DNA polymerase. All 30 pairwise combinations of primers were used. Reactions were placed in a Perkin-Elmer 480 thermal cycler (Applied Biosystems, Inc., Foster City, CA) at 94°C (3 min) and then cycled 25–40 times at 96°C (45 s), 47°C (144 s) or 53°C (216 s), and 72°C (3 min, 6 s extension/cycle). Products were T/A cloned (53), screened by in situ hybridization, and sequenced. The product used to clone *vzg-1* ("513") was independently isolated using TM II primer 5'AA(C/T)T(A/G)(C/G)ATI(A/C)TI(C/G)TIAA(C/T)(C/T)TIGC-IGTIGCIGA and TM VII primers 5'CTGI(C/T)(G/T)(A/G)TTCATIA(A/T)I(A/C)(A/C)(A/G)TAIA(C/T)IA(C/T)IGG(A/G)TT, 5'TCIAT(A/G)-TT(A/G)AAIGTIGT(A/G)TAIATIATIGG(A/G)TT, and 5'AA(A/G)TCIGG(A/G)(C/G)(A/T)ICGI(C/G)A(A/G)TAIAT(C/G)AIIGG(A/G)T T.

Full-Length Vzg-1 cDNA Cloning. Clone "513" was used to screen 500,000 phage plaques at high stringency from a postnatal day 20 BALB/c (same strain as cell lines TR and TSM) mouse brain library (Stratagene, La Jolla, CA). Clone "pSt3," containing a 2,250-bp insert, was sequenced

completely in both directions by the dideoxy chain termination method (2). Sequence analysis used BLAST (NCBI, Bethesda, MD), MacDNAsis (Hitachi Software, San Bruno, CA), and the GCG programs (Genetics Computer Group, Madison, WI).

Expression Vectors. Vectors for transfection contained the 1,131-bp Ear I-Nae I *vzg-1* open reading frame fragment from pSt3 in the sense or antisense orientation, blunt-end cloned into the EcoRV site of pcDNAI/Amp (InVitrogen, San Diego, CA) by standard protocols (2). Thrombin receptor expression vector (37) was kindly provided by Dr. S. Coughlin (University of California San Francisco).

RNA Isolation and Northern Analysis. These methods have been previously described (2, 14, 19).

Histology

In Situ Hybridization. In situ hybridization to BALB/c mouse embryos was performed as previously described using digoxigenin-labeled riboprobes visualized by alkaline phosphatase histochemistry (19, 73).

BrdU/In Situ Hybridization Double Labeling. Timed pregnant BALB/c mice were injected intraperitoneally with 20 μl 10 mM BrdU/g body weight 1 h before sacrifice. In situ hybridization and probe visualization were immediately followed by HCl incubation (60°C in 1 N HCl, 15 min), and slides were washed in PBS (RT, 10 min, 3×), incubated in blocking solution (RT, 2.5% BSA, 0.3% Triton X-100, 1× PBS, 1 h), and then incubated in 6 μg/ml mouse monoclonal anti-BrdU antibody (RT, 1 h) (Boehringer-Mannheim Corp., Indianapolis, IN). Bound antibody was visualized by anti-mouse Vectastain ABC peroxidase kit (Vector Laboratories, Burlingame, CA) as previously described (15–18).

Phospholipid Sources and Receptor–Ligand Binding

Lipids (1-oleoyl-lysophosphatidylethanolamine [LPE], 1-oleoyl-lysophosphatidylglycerol [LPG], 1-oleoyl-lysophosphatidylcholine [LPC], 1, 2-dioleoyl-phosphatidic acid [PA], 1-stearoyl-LPA, and 1-oleoyl-LPA) were obtained from Avanti Polar Lipids (Alabaster, AL). Labeled ligand (1-oleoyl-[9,10-^{3}H]-LPA; Dupont/NEN, Boston, MA) was prepared by evaporating >50% of the solvent under a N$_2$ stream and reconstituting the volume with 100% ethanol. All lipids were synthetic, 98–99% pure.

Membrane Isolation and [^{3}H]LPA Binding Assay. Cell lines were grown to 90% confluence, washed with PBS, scraped from the plate, centrifuged for 5 min (110 g), washed with PBS, recentrifuged, and the pellet then resuspended in 10 ml of ice-cold 20 mM Tris, pH 7.5, disrupted by 20 strokes in a glass homogenizer, and sonicated on ice with three 10-s bursts using a microultrasonic cell disrupter (Kontes Glass, Hayward, CA). After low speed centrifugation (1,000 g, 15 min, 4°C), membranes were pelleted from the supernatant (16,000 g, 30 min, 4°C), and resuspended at 3 μg/μl protein in ice-cold 20 mM Tris, pH 7.5. Just before analysis, membranes were resonicated for 5 s on ice until the solution became transparent, then LPA binding assays carried out as previously described (71). Briefly, binding reactions (500 μl of 50 μg/ml membrane protein in an assay buffer of 20 mM Tris, pH 7.5, and 0.5 mM CuSO$_4$) were initiated by addition of 1-oleoyl-[9,10-^{3}H]-LPA (56.2 Ci/mmol) to a final concentration of 8.5 nM (230,000 cpm) and incubated (30°C, 30 min). To assess nonspecific binding, 2 μM unlabeled 1-oleoyl-LPA was added to a set of parallel reactions. Reactions were run through PD-10 Sephadex G25M columns (Pharmacia LKB Biotechnology) to separate bound from free ligand. The eluent (1.5 ml) was mixed with scintillation fluid (Ultima Gold; Packard Instrument Co., Inc., Meriden, CT) and counted at RT. About 5–10% of the total input cpm were collected in the eluent. Uncorrected total binding ranged from 13,000 to 20,000 cpm. Because LPA forms aggregates that are excluded from the column bed and thus collected in the eluent, each experiment was performed in parallel using reactions without membranes, in the presence or absence of 2 μM LPA, to determine eluted background cpm. Total and nonspecific cpm were corrected by subtraction of the appropriate background cpm. Specific cpm were calculated by subtracting corrected nonspecific cpm from corrected total cpm. Overall, with correction, nonspecific cpm were 61% of total cpm. Experiments were done in triplicate and the results statistically analyzed using Student's *t*-test.

Antiserum Production and Western Blot Analysis

A rabbit polyclonal antiserum was raised against Vzg-1 by cDNA vaccination (25, 60). Twice weekly intradermal injections of *vzg-1* expression construct (20 μg) in PBS for 6 wk were followed by a week hiatus (test bleed) and then injections repeated for 4 wk and serum collected. Cells were se-

a
```
  1 GAATTCGGCACGAGGCACAGTGCTGCCCTCCGTAGGCTCCGGGTTGTGCTGGGGTGAGGCTTGGGTTGGGTTGGCCCGGCGGCTGCGTGAACTGCGGAGC
101 TGGACCTAGCAGGCTTACAGTTCCTCCTAGCATGACCGAGATCTGATCAGCCAACCCGCGCATTGCTTTTTGTGCCTGGCACTGCAGTGCAGGGGGCCTC
201 TTCATCGCCCCAAACTACAGCACTGTC
```

```
  1 M  A  A  A  S  T  S  S  P  V  I  S  Q  P  Q  F  T  A  M  N  E  Q  Q  C  F  Y Ⓝ E  S  I  A  F  F
228 ATGGCAGCTGCCTCTACTTCCAGCCCTGTAATTTCACAGCCCCAGTTCACAGCCATGAACGAACAACAGTGCTTCTACAATGAGTCTATCGCCTTCTTT

 34 Y Ⓝ R  S  G  K  Y  L  A  T  E  W  N ┌T  V  S  K  L  V  M  G  L  G  I  T  V  C  V  F  I  H  L  A┐   TM I
327 TATAACCGGAGTGGGAAATATCTAGCCACAGAATGGAAC ACAGTGAGCAAGCTGGTGATGGGACTGGGCATCACTGTTTGCGTGTTCATCATGTTGGCC

 67 ┌N  L  L  V┐ M  V  A  I  Y  V  N  R  R ┌F  H  P  P  I  Y  Y  L  M  A  N  L  A  A  A  D  F  F  A  G┐  TM II
426 AATCTCCTGGTCATGGTGGCAATCTACGTCAACCGCCGCTTCCATTTCCCTATTTATTACTTGATGGCCAACCTGGCTGCTGCAGACTTCTTCGCTGGA

100 ┌L  A  Y  F  Y  L┐ M  F  N  T  G  P  N  T  R  R  L  T  V  S  T ┌W  L  L  R  Q  G  L  I  D  T  S  L┐
525 TTGGCCTACTTCTACCTGATGTTCAATACAGGACCTAATACCCGGAGACTGACTGTTAGCACGTGGCTCCTCCGGCAGGGCCTCATTGACACCAGCCTG

133 ┌T  A  S  V  A  N  L  L  A  I  A  I┐ E  R  H  I  T  V  F  R  M  Q  L  H  T  R  M ┌S  N  R  R  V  V┐   TM III
624 ACAGCTTCTGTGGCCAACCTGCTGGCTATTGCTATCGAGAGGCACATCACGGTTTTCCGCATGCAGCTCCATACACGAATGAGCAACCGGCGCGTGGTG

166 ┌V  V  I  V  V  I  W  T  M  A  I  V  M  G  A  I  P┐ S  V  G  W  N  C  I  C  D  I  D  H  C  S  N  M    TM IV
723 GTGGTGATTGTAGTCATCTGGACTATGGCCATTGTGATGGGTGCTATACCCAGTGTGGGCTGGAACTGCATCTGTGATATCGATCACTGTTCCAACATG

199 A  P  L  Y  S  D ┌S  Y  L  V  F  W  A  I  F  N  L  V  T  F  V  V  M  V  V  L┐ Y  A  H  I  F  G  Y     TM V
822 GCACCCCTCTACAGTGACTCCTACTTAGTCTTCTGGGCCATTTTCAACCTGGTGACCTTTGTGGTCATGGTGGTTCTCTACGCTCACATCTTTGGCTAT

232 V  R  Q  R  T  M  R  M  S  R  H  S  S  G  P  R  R  N  R  D  T  M  M  S ┌L  L  K  T  V  V  I  V  L┐
921 GTTCGCCAGAGGACTATGAGGATGTCTCGGCATAGTTCTGGACCCAGGAGGAATCGGGACACCATGATGAGCCTTCTGAAGACTGTGGTCATTGTGCTT

265 ┌G  A  F  I  V  C  W  T  P  G  L  V  L  L  L  L┐ D  V  C  C  P  Q  C  D  V ┌L  A  Y  E  K  F  F  L┐   TM VI
1020 GGTGCCTTTATTGTCTGCTGGACTCCGGGATTGGTCTTGTTATTGCTGGATGTGTGCTGCCCGCAGTGCGATGTCCTGGCCTATGAGAAGTTCTTCCTC

298 ┌L  L  A  E  F  N  S  A  M  N  P  I  I┐ Y  S  Y  R  D  K  E  M  S  A  T  F  R  Q  I  L  C  C  Q  R    TM VII
1119 CTCCTGGCCGAGTTCAACTCTGCTATGAACCCCATCATCTACTCCTACCGCGACAAAGAGATGAGCGCCACCTTCAGGCAGATCCTGTGTTGCCAGCGC

331 N  E  N  P  N  G  P  T  E  G  S  D  R  S  A  S  S  L  N  H  T  I  L  A  G  V  H  S  N  D  H  S  V
1218 AACGAGAACCCTAATGGCCCCACGGAAGGCTCTGACCGCTCTGCCTCCTCCCTCAACCACACCATTCTGGCTGGAGTTCACAGCAACGACCACTCTGTG

364 V  *
1317 GTTTAG
```

```
1323 AAGGAAGCCAGCCGGCCTCTGTGGATCTGTGAACCCCACCCTACCCCCCATTGCCAGGGCAAGGTGGGGAGCCAGAGGAGATGAGGACACTCCTGTACTT
1423 AACACTAACCAATGGCAGTATTTGTCCCTAGACCCAAGAGACTTGAGGATGAATTTATTTGGCAGGCCCCATCTTCTCCTTTGGAAAACAGAAGGGGACC
1523 GTCTTGTGGTGGAATTGAGAAATGGACTCTGGGGTGACCGTGTAGCATTCACTAACTAGACTTAAAAGATTTTATGTGGTTTGGCTTAAGCCAGGAAAAA
1623 AAAATCTGCTGAATTGAGTATACAATCGAGTATACACAGGCTTCCCCTTTAAAGAACAAACAATACATTGCATTTATTAATGAGTATGTTTATGCCTGAC
1723 AGCATGTTTGTGATCGAAAAGACTGCTAAACTGACATAGATGAGTTGTTTTTTTTTTTTTTGTTTTTTGTTTTTTTTTACATGATGGAGGAAAAGTATAAA
1823 TTAGAATGATTTTTGTGTTTTGTTTAGAAAGCAAGCATGTGGTGTGTGTATTCAGTATGCCTTTCTTTAAAGATAAAAGGCCACTATTTTAAATCTTCTAG
1923 GGAATAGAAGAATCTAGTAAAAACCAGTATTCATTTAGGCTACAGGAAAAACCATATCCTAATCAATTACCTTTTAATTAAAGTAATGAAATATACATGA
2023 AAGGCAAAGTAATGTGAGCTTGTCACCCAAAGAGTGTGTGCTCTCCAAACGCTGGAGGAGATGAAGCTGTAGCGTTGTCCCTGCATAGTGAAGATACCCA
2123 CGTGCGTTCTCAGTGCCAGACCCTCAGTGGGACTTGTTTTAAAGCCTGTGGTTTTCCAAGTTAGAAAATAATACCTACTTACTATAGAAAACTTGAAAAT
2223 TGCAGAACTGTGTGAAAAAAAAAAAAAAAA
```

b

Figure 2. Vzg-1 encodes a GPCR. (*a*) Nucleotide and predicted aa sequences of *vzg-1*. The 2,250-bp sequence contains a 1,095-bp open reading frame, extending from bases 228–1322, (*, stop codon). There are two in-frame stop codons located 5' to the translational start site at positions 33 and 144 of the nucleotide sequence. Positions of TM domains I through VII are boxed (see *b*). Vzg-1 has conserved aa residues shared amongst many members of the GPCR family (v) (57). Other common features are N-linked glycosylation sites (*circled*) (24, 59), cysteine residues that may form disulfide bonds (*overlined*) (42), and cysteine residues that can potentially be lipid-modified (●) (80). Multiple serine and threonine residues in the third intracellular loop and COOH-terminal intracellular domain are potential sites for regulatory phosphorylation (31). These sequence data are available from GenBank/EMBL/DDBJ under accession number U70622. (*b*) Kyte-Doolittle hydrophobicity analysis of Vzg-1 (46) reveals seven putative TM domains. Positive values indicate hydrophobicity, while negative values indicate hydrophilicity. The plot was calculated using a window of 15 aa.
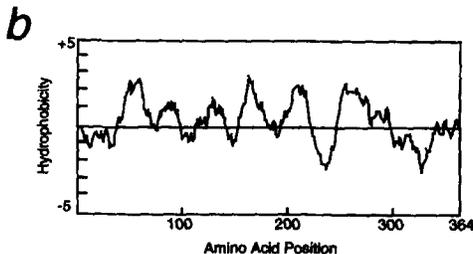
rum starved 24 h and membranes were prepared as above, except that buffers contained 1 mM EGTA, 1 mM PMSF, and 1 mM benzamidine. Western blot techniques were as previously described (15, 16). Briefly, membrane proteins were solubilized in 1X sample buffer (2), separated on 15% SDS-PAGE minigels, electroblotted onto nitrocellulose (Schleicher & Schuell, Inc., Keene, NH), and incubated overnight (RT) with 1:100 dilution of primary antiserum. Bound antibody was detected using the Vectastain ABC kit (Vector Laboratories, Burlingame, CA) using DAB visualization.

Results

Vzg-1 Encodes a Novel Seven-Transmembrane Domain Molecule

Degenerate oligonucleotide primers against amino acid (aa) sequences from TM II and TM VII of the GPCR family (7, 48) were used in PCR amplification of neocortical cell line cDNA (lines TR and TSM (14); Materials and Methods). A total of 154 DNA fragments representing 58 distinct PCR products in the expected size range from 600

to 1,300 bp were cloned. One fragment, "513," was localized to the vz (Fig. 1 *b*) by in situ hybridization and was represented by 13 independently derived clones having GPCR aa sequence homology. Northern blot analysis of embryonic brain detected a single 3.8-kb transcript. Library screening led to isolation of a 2.4-kb cDNA, termed *vzg-1*, containing an open reading frame (Fig. 2 *a*) encoding a 41-kD protein with seven hydrophobic membrane spanning domains (Fig. 2 *b*), as well as other features of the GPCR family. Comparisons to published sequences (data not shown) demonstrated that Vzg-1 shared homology with the melanocortin receptor (32% aa identity) (23), cannabinoid receptor (30% aa identity) (52), and the orphan receptor gene *edg-1* (37% aa identity) (36).

Vzg-1 Expression Correlates with Cortical Neurogenesis

The full-length *vzg-1* clone hybridized to a transcript iden-
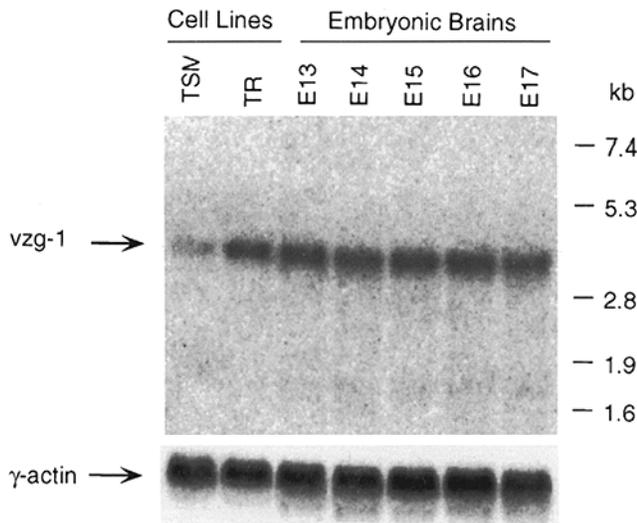
Figure 3. *Vzg-1* is expressed in the embryonic mouse brain and in neocortical neuroblast cell lines. Total RNA (10 μg) from mouse brains at E13–E17 and cytoplasmic RNA from cell lines TSM and TR were analyzed by Northern blot analysis using a *vzg-1* probe. The *vzg-1* transcript is 3.8 kb (γ-actin loading control is shown).

tical in size to that identified by fragment 513, which was present in the embryonic mouse brain and in the cell lines from which it was cloned (Fig. 3). *Vzg-1* expression was examined in mouse embryos from E12 to E18 by in situ hybridization. A low magnification view (shown for E14) demonstrated that, within the CNS, *vzg-1* expression was highly enriched within the cerebral cortical vz in the dorsal telencephalon. Additional hybridization is observed to a tissue layer closely apposed to CNS, likely to be a developing meningeal layer (Fig. 4, *a* and *b*).

Vzg-1 was expressed throughout most of the cerebral wall at E12, when it consists mainly of proliferative neuroblasts (Fig. 5). As this wall thickens with further development, *vzg-1* expression remained primarily restricted to the proliferative vz (Fig. 5; see also Fig. 1 *b*). The *vzg-1* hybridization signal appeared most intense at E12 and E14, somewhat less at E16, and was barely detectable at E18. Thus, *vzg-1* expression is primarily restricted to the vz of the cerebral cortex during neurogenesis.

Vzg-1 Overexpression Induces Sustained, LPA-dependent Cell Rounding

To determine possible functions of *vzg-1*, cell line TSM, chosen for its comparatively low expression of the endogenous transcript (Fig. 3), was transiently transfected with expression vectors containing *vzg-1* in the sense or antisense orientation. Transfection with the *vzg-1* sense expression vector induced neurite retraction and cell rounding, which was maintained for at least 24 h (Fig. 6 *a*, "sustained cell rounding"). This morphological change required the presence of serum. Sense transfected cells exposed to serum had 48 ± 3.6% round morphology, compared to 22 ± 5.0% without serum (Table I).

The reproducibility of cell rounding allowed its use as a bioassay to identify putative ligands for *vzg-1*. Boiling the serum did not abolish its ability to mediate cell rounding (data not shown), indicating that the ligand was a heat sta-

ble molecule that might be associated with (*a*) cytoskeletal changes and (*b*) cell proliferation, since *vzg-1* expression was restricted to the vz. A molecule present in serum that met these criteria (see Discussion) was LPA. Since endogenous Vzg-1 should be active in the cell lines from which it was identified, untransfected TSM cells were first assayed for their ability to respond to LPA. Indeed, TSM cells responded with a rapid increase in the percentage of round cells. However, this response was reversible such that by 3 h, the percentages of round cells returned to their baseline values (Fig. 6 *b*).

Transfection of TSM cells with *vzg-1* in the sense orientation sustained the rounding response to LPA such that at 3 h, 49 ± 4.9% of treated transfected cells still displayed a round morphology, compared to 29 ± 1.9% of untreated transfected cells (Table I). Importantly, thrombin, a serum component which also induces cell rounding in some neural cell lines (38, 66), did not induce sustained cell rounding in cells transfected with *vzg-1*, although it did induce sustained cell rounding in cells transfected with the thrombin receptor (Table II). Thus, transient overexpression of *vzg-1* specifically alters LPA-mediated changes in cell morphology.

Vzg-1 Overexpressing Cell Lines Show Morphological Responses Specific to LPA

Vzg-1 function was characterized in TSM cells stably transfected with the *vzg-1* sense construct, using the antisense construct and empty vector as transfection controls. (Stably transfected cell lines will be referred to as "sense, empty vector, or antisense cells.") Overexpression of *vzg-1* in sense cells was at least fivefold over endogenous expression, and in antisense cells at least twofold over endogenous expression, determined by Northern analysis and scanning densitometry (data not shown). Vzg-1 protein in sense cells (line *3*) was overexpressed relative to empty vector (line *33*) or antisense (line *17*) cells (Fig. 7 *a*). Sense cells, but not empty vector or antisense cells, responded to LPA by sustained cell rounding at 3 h (Fig. 7 *b*).

The specificity of the LPA response in *vzg-1* sense cells was tested using a range of structurally related phospholipids. Two forms of LPA, 1-oleoyl-LPA and 1-stearoyl-LPA, were examined along with four other structurally related lipids: 1-oleoyl-LPC, 1-oleoyl-LPE, 1-oleoyl-LPG, and 1, 2-dioleoyl-PA (Table III). Compared to the other phospholipids, only LPA lipids produced sustained cell rounding after 3 h of treatment, and thus the response was specific to LPA.

Vzg-1 Overexpression Decreases the EC_{50} of LPA-induced Cell Rounding

The cell rounding bioassay was used to determine the effect of LPA concentration on sense, antisense, and empty vector cells. Concentration-response experiments defined the EC_{50}, minimal, and maximal response values of the morphological response to LPA (Fig. 7 *c* and Table IV). Sense cells displayed a similar maximal response to LPA as empty vector cells, but were 6.9-fold more sensitive, as demonstrated by a shift in the concentration-response curve to the left. In contrast, antisense cells displayed decreased basal and maximal responses but equal sensitivity
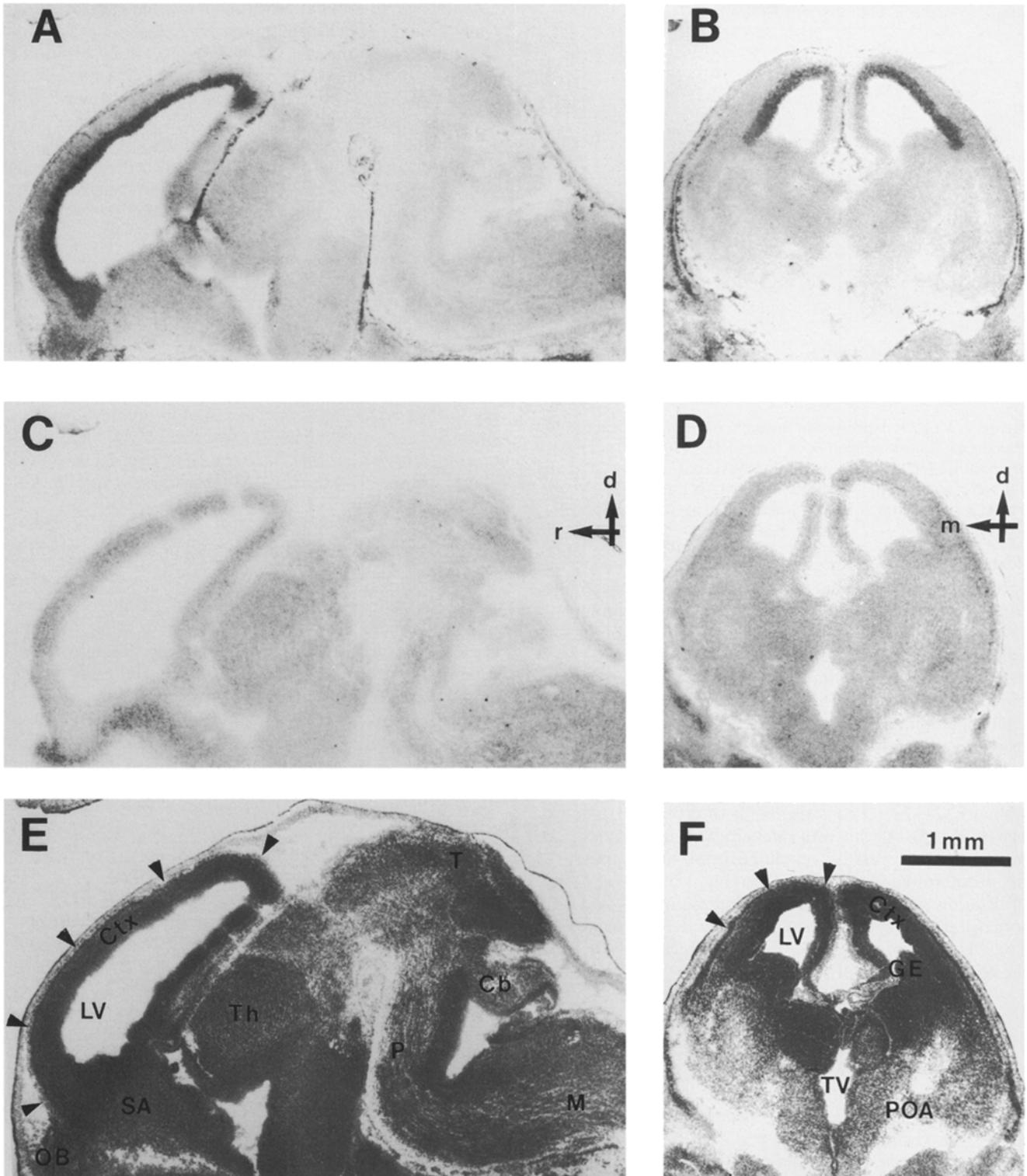
Figure 4. Vzg-1 expression in the embryonic CNS is enriched within the vz. Low magnification view of adjacent sagittal (*a, c,* and *e*) and coronal (*b, d,* and *f*) sections of E14 mouse embryo hybridized to antisense (*a* and *b*) or sense control (*c* and *d*) digoxigenin-labeled ribo-probes, or stained with cresyl violet (*e* and *f*). The hybridization pattern produced by the antisense probe is restricted to the neuroprolif-erative vz of the embryonic cortex. *Ctx,* cortex; *LV,* lateral ventricle; *OB,* olfactory bulb; *SA,* striatum; *Th,* thalamus; *T,* tectum; *P,* pons; *Cb,* cerebellum; *M,* medulla; *GE,* ganglionic eminence; *TV,* third ventricle; *POA,* preoptic area; *d,* dorsal; *r,* rostral; *m,* medial. Bar, 1 mm.
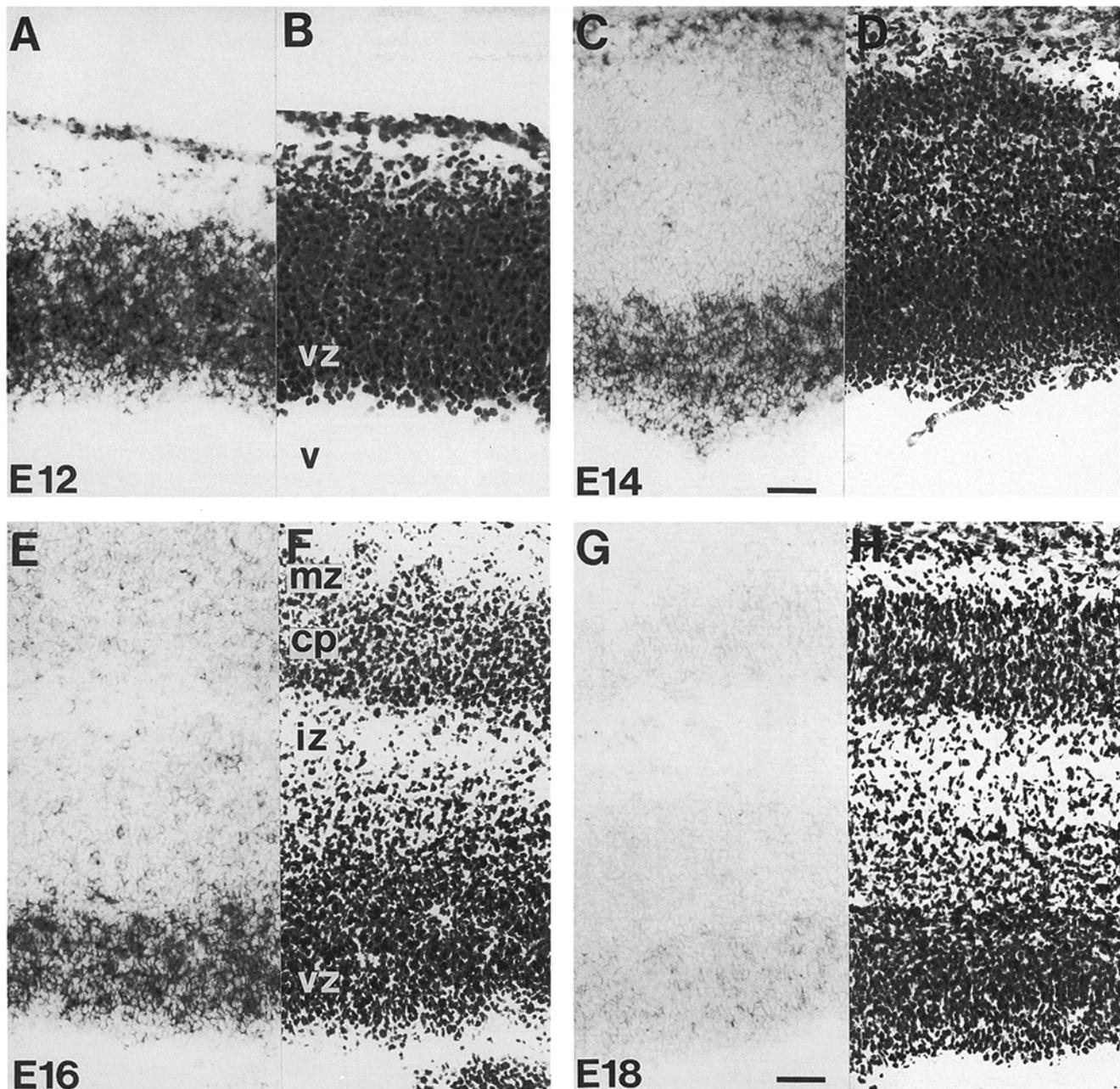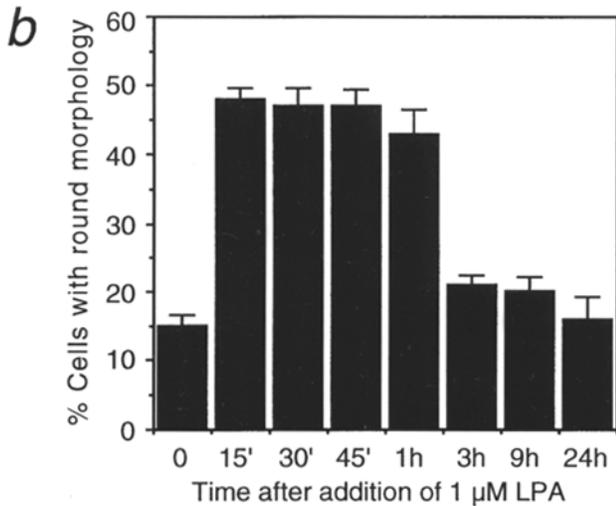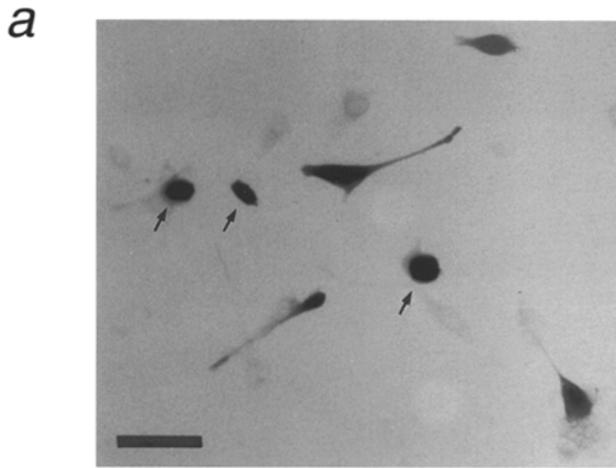
Figure 5. Developmental expression of *vzg-1* parallels the anatomical location and period of cortical neurogenesis. Sagittal sections of the cortex from E12–E18 hybridized to antisense *vzg-1* riboprobe (*a, c, e,* and *g*) compared to an adjacent section stained with cresyl violet (*b, d, f,* and *h*). *Vzg-1* expression is largely confined to the vz throughout this period. *Vzg-1* appears highly expressed at E12 and E14, less so at E16 and at minimal levels at E18. *vz,* ventricular zone; *iz,* intermediate zone; *cp,* cortical plate; *mz,* marginal zone; *v,* ventricle. Bar, 50 µm.

as control cells. Two other sets of independently derived cell lines showed similar results (data not shown). Thus, overexpression of the sense *vzg-1* construct specifically increased the potency of LPA, a result consistent with *vzg-1* encoding a receptor for LPA.

Vzg-1 Overexpression Decreases the EC₅₀ of LPA-stimulated Gᵢ Activation

To examine whether *vzg-1* overexpression altered LPA-mediated G_i activation, sense, antisense, and empty vector cells were tested for LPA-stimulated inhibition of cAMP accumulation. As shown in Table IV, the EC_{50} in sense cells was reduced 6.6-fold relative to empty vector cells. Antisense cells had a similar EC_{50} as empty vector cells. The effect of LPA on cAMP accumulation was reversed by PTX treatment, indicating activation of G_i; however, PTX treatment did not affect LPA-induced cell rounding (Table V). The effect of *vzg-1* on LPA-mediated G_i activation was specific to LPA since adenylate cyclase inhibition

a

Table I. Serum and LPA Induce Sustained Cell Rounding in TSM Cells Transiently Transfected with Vzg-1

Expression vector	5% FCS (percent round, mean ± SEM)		1 µm LPA (percent round, mean ± SEM)	
	+	−	+	−
Vzg-1 sense	48 ± 3.6*	22 ± 5.0	49 ± 4.9*	29 ± 1.9
Control: vzg-1 antisense	20 ± 0.88	23 ± 2.2	27 ± 2.1	24 ± 1.3
Control: empty vector	21 ± 6.0	23 ± 4.2	ND	ND

Cells were transiently transfected with the indicated expression vectors, followed by treatment with either FCS for 24 h or LPA for 3 h. Data represent the mean ± SEM for three to four independent experiments, each done in duplicate.
*Indicates statistically significant differences from control conditions (P < 0.001).

terials and Methods). Nevertheless, [³H]LPA binding assays were performed on membrane preparations from sense and antisense cells to determine whether overexpression of *vzg-1* increased the number of specific [³H]LPA binding sites. Membrane preparations derived from sense cells showed a statistically significant increase in specific [³H]LPA binding compared to membranes from antisense lines (Fig. 7 *d*). This result demonstrated that *vzg-1* overexpression is associated with an increase in the number of binding sites for [³H]LPA.

Adult Expression of Vzg-1 Parallels Prior Estimates of LPA Receptor Distribution

Prior studies examining the distribution of LPA receptors demonstrated that in adult tissues, receptors are present at very high levels in the brain, are virtually absent from the liver, and are present at intermediate levels in other tissues (71, 77). Additionally, high levels of receptor are expressed in NIH-3T3 cells. Northern blot analysis (Fig. 8) demonstrated that *vzg-1* was expressed at maximal levels in the adult brain, absent from liver, and present at intermediate levels in other tissues, a pattern paralleling these previous results. *Vzg-1* was also highly expressed in NIH-3T3 cells (data not shown).

b

Figure 6. LPA induces cell rounding and neurite retraction in TSM cells. (*a*) Transfected cells, identified by β-galactosidase staining, either have round morphologies (*arrows*) or pyramidal or bipolar morphologies. Bar, 50 µm. (*b*) LPA response of untransfected TSM cells. Within 15 min, LPA caused an increase in the proportion of round cells. Note that the proportion of round cells returns to baseline after 3 h, allowing transfection experiments to be carried out on this time scale. Values represent the mean ± SEM of three independent experiments, each done in duplicate.

mediated by UK14304, an α₂-adrenergic receptor agonist, did not show differential effects on sense and antisense overexpressing cells (data not shown).

Vzg-1 Overexpression Increases LPA Binding in Cell Membranes

The use of binding assays with [³H]LPA to study ligand-receptor interactions is complicated by the lipophilic and detergent properties of LPA (26, 71, 74, 77), resulting in substantial nonspecific and background binding (see Ma-

## Discussion

LPA Meets Criteria Expected for a Vzg-1 Ligand

Functional analyses of *vzg-1* required ligand identification, a difficulty underscored by the huge variety of molecules recognized by the GPCR family (80). Ligand identification was aided by three observations from our study. First, *vzg-1*

Table II. LPA, but Not Thrombin, Stimulates Vzg-1–dependent Sustained Cell Rounding

Expression vector	1 µM LPA (percent round, mean ± SEM)	0.5 U/ml thrombin (percent round, mean ± SEM)	Control: no treatment (percent round, mean ± SEM)
Vzg-1 sense	47 ± 2.2*	23 ± 4.1	23 ± 4.3
Thrombin receptor	32 ± 2.0	76 ± 2.1*	28 ± 2.3

TSM cells were transiently transfected with the indicated expression vectors followed by treatment with either LPA for 3 h or thrombin for 2 h. Data represent the mean ± SEM for three independent experiments, each done in duplicate.
*Indicates statistically significant differences from control conditions (P < 0.001).
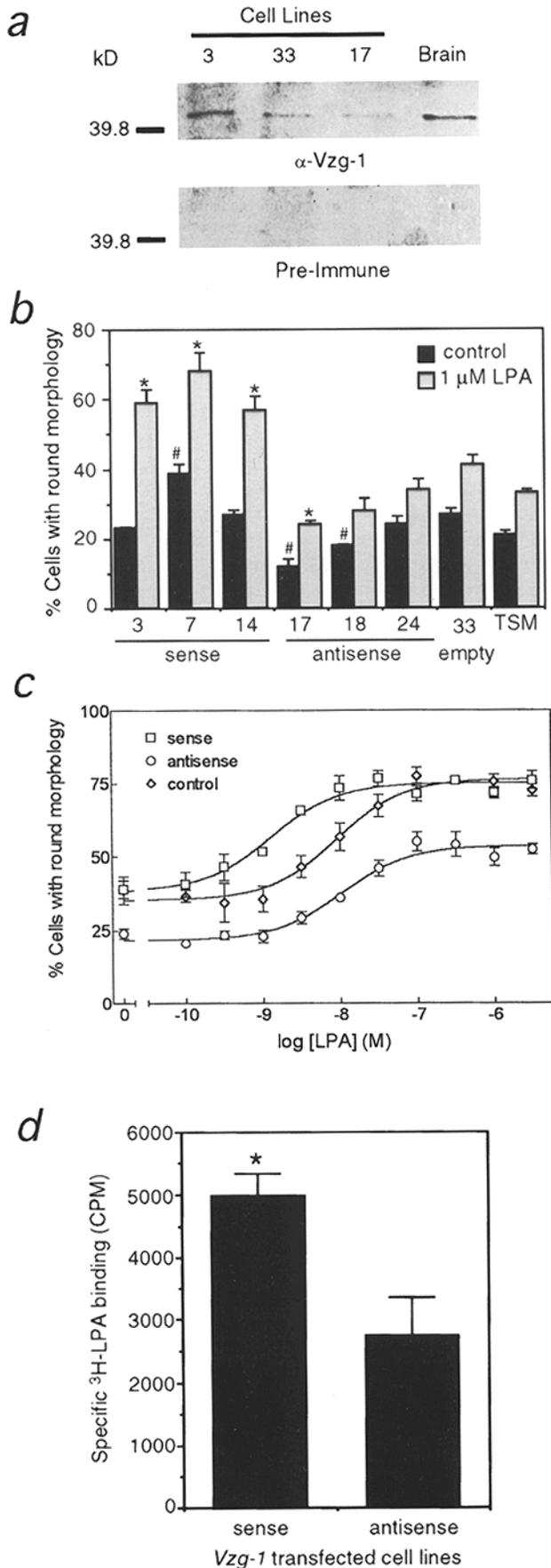
was highly expressed in the vz, suggesting a function in some aspect of cortical neurogenesis (see below). Second, *vzg-1*–dependent, serum-induced, sustained cell rounding was highly reproducible, allowing its use as a bioassay. Third, the serum factor inducing cell rounding was heat stable. Prior studies reported that cortical blast proliferation required (a) cell membrane extracts or cell–cell contact (30, 69) and (b) serum (43, 70). Thus, ligand(s) for Vzg-1 could (a) be involved in cell proliferation or differentiation, (b) promote morphological changes like cell rounding, (c) be heat stable, and (d) be a component of serum or cell membrane extracts.

All of these criteria were met by the bioactive lipid LPA (54). LPA is mitogenic for nonneural cells (72, 75, 81, 82), produces actin-based stress fiber formation in fibroblasts (61), and results in the retraction of "neurites" and cell rounding in neuroblastoma-derived cell lines (40). It is a heat-stable component of serum (61), present at a concentration of 2–20 μM, that is bound to albumin (27). It can also be produced from cell membrane phospholipids by phospholipase A2 (29).

Vzg-1 Has Predicted Properties of a Receptor for LPA

The *vzg-1* gene product meets the expected criteria of a receptor for LPA. *Vzg-1* encodes a GPCR based on se-

Figure 7. Vzg-1 sense overexpression enhances LPA-induced cell rounding and increases [³H]LPA binding to cell membranes. (a) Vzg-1 sense strand–transfected cell lines express more protein than control cells. Sense-transfected cells (shown for line 3) expressed more Vzg-1 than empty vector (33) or antisense (17) cells, using an α-Vzg-1 antiserum that specifically detects a 41–42-kD protein not detected by preimmune serum. An identically sized protein is detected in adult brain. Equivalent amounts of membrane protein (5.5 μg) were loaded in each well as determined by Bradford assay of the sample, and confirmed by Coomassie staining after gel electrophoresis (data not shown) (2). (b) Response of stably transfected cell lines after 3 h treatment with 1 μM 1-oleoyl LPA. Cell lines stably transfected with the sense *vzg-1* expression construct (lines 3, 7, and 14) showed enhanced responses to LPA compared to empty vector control line 33. Antisense cell lines (lines 17, 18, and 24) have lower responses to LPA than the empty vector control line 33. * indicates statistically significant differences between experimental cells and control line 33 in the presence of LPA, with individual pairwise P values ranging from P < 0.05 to P < 0.001. # indicates statistically significant differences between experimental cells and control line 33 without LPA stimulation, with individual pairwise P values ranging from P < 0.05 to P < 0.001. All values represent the mean ± SEM of three to five independent experiments, each done in duplicate. (c) Concentration-response relationship of stably transfected cells to a three to five min treatment with LPA. Sense transfected cells show an increased sensitivity to LPA compared to empty vector control cells as demonstrated by a leftward shift of the EC_{50}. Antisense transfected cells have identical EC_{50} as controls, but lowered minimal and maximal responses (Table IV). Curves were fitted to data points representing the mean ± SEM of three independent experiments, each done in duplicate. (d) Vzg-1 overexpression results in increased [³H]LPA binding in membranes from sense-transfected cells (shown for line 3), compared to membranes from antisense-expressing cells (shown for line 17). * indicates a significant difference from control (P = 0.021), data expressed as the mean ± SEM of four experiments, done in triplicate.

Table III. LPA Specifically Induces Vzg-1–dependent and Sustained Cell Rounding

Phospholipid	Line 3 (percent round, mean ± SEM)	Line 7 (percent round, mean ± SEM)	Line 14 (percent round, mean ± SEM)
1-Oleoyl LPA	50 ± 2.3*	57 ± 2.8*	54 ± 1.3*
1-Stearoyl LPA	33 ± 1.2	55 ± 3.1*	35 ± 2.6*
1-Oleoyl LPE	29 ± 1.3	44 ± 1.1	27 ± 1.1
1-Oleoyl LPG	22 ± 0.71	37 ± 1.2	25 ± 0.85
1-Oleoyl LPC	24 ± 2.5	42 ± 2.0	29 ± 0.25
1,2-Dioleoyl PA	27 ± 1.0	43 ± 0.85	31 ± 2.1
Control: medium alone	27 ± 2.8	39 ± 1.7	24 ± 1.6

Cell lines stably transfected with the *vzg-1* sense construct were serum deprived for 24 h, and then treated with 1 μM concentrations of the indicated phospholipids for 3 h. Data represent the mean ± SEM for four independent experiments, each done in duplicate.
*Indicates statistically significant differences from control conditions ($P < 0.01$ to $P < 0.001$)

Table V. LPA-induced Adenylate Cyclase Inhibition, but Not Cell Rounding, is Blocked By PTX

Treatment	cAMP percentage of maximum response (mean ± SEM)	Percent round cells (mean ± SEM)
Control: medium alone	100	40 ± 3.2
LPA	45 ± 3.4*	77 ± 2.1*
LPA + PTX	84 ± 5.0	81 ± 3.5*

Vzg-1 sense overexpressing cells (cell line 3) were serum deprived 24 h and then stimulated with 100 nM LPA for 7 min for cAMP assays or with 50 nM LPA for 15 min rounding assays. Data represent the mean ± SEM for three independent experiments done in triplicate for cAMP assays or duplicate for rounding assays.
*Indicates statistically significant differences from control conditions ($P < 0.001$)

quence homology (57). The ability of this receptor to bind [³H]LPA was tested using membrane binding assays. Binding studies with LPA are complicated by the lipophilic detergent properties of the radioligand, which favor partitioning into phospholipid bilayers and micelle formation, resulting in substantial levels of nonspecific binding, inefficient separation of bound ligand from free, and high levels of background. As a result of these technical limitations, binding assays cannot be used to make quantitatively rigorous measurements of LPA binding sites, as noted in previous studies (26, 71, 74, 77). Because of these biophysical properties of LPA and the lack of specific antagonists (77), we cannot pharmacologically characterize LPA interaction with Vzg-1. However, *vzg-1* overexpression was associated with a statistically significant increase in specific [³H]LPA membrane binding, a result consistent with the functional characterization of *vzg-1* as a receptor for LPA.

In TSM neuroblast cell lines overexpressing *vzg-1*, LPA induced specific, sustained neurite retraction and cell rounding, as reported previously in neuroblastoma cell lines (39). Neither other phospholipids nor thrombin produced *vzg-1*–dependent, sustained cell rounding. Characterization of LPA signaling pathways in *vzg-1* overexpressing cell lines revealed a *vzg-1*–dependent enhancement of LPA signaling reflected by a decrease in the EC₅₀ of LPA-induced, Gᵢ-independent cell rounding and Gᵢ-dependent inhibition of cAMP formation, as predicted by previous

studies (39, 74). Based on receptor theory (56), the increase in potency seen with sense cells is most simply explained by an increase in receptor number, consistent with the increase in protein levels detected by Western blot analysis (Fig. 7 *a*). Prior studies on LPA receptor distribution implicated a 38–40-kD protein highly expressed in the adult brain and absent from liver (71, 77). *Vzg-1* tissue distribution parallels these prior estimates, and, furthermore, *vzg-1* encodes a predicted protein of consistent size (41 kD), confirmed by anti–Vzg-1 Western blot analysis.

Therefore, seven different lines of evidence identify the *vzg-1* gene product as a lysophosphatidic acid receptor: (*1*) identification of *vzg-1* as a GPCR gene, (*2*) *vzg-1*–dependent increases in specific [³H]LPA membrane binding, (*3*) *vzg-1*–dependent decrease of the EC₅₀ for Gᵢ-independent LPA-mediated cell rounding, (*4*) *vzg-1*–dependent decrease of the EC₅₀ of LPA-mediated activation of Gᵢ, (*5*) correspondence between the predicted size of the *vzg-1* gene product and prior estimates of LPA receptor size, (*6*) detection of a gene product of the correct size in brain, with increased levels of expression in sense transfected cells, and (*7*) correlation between tissue expression of *vzg-1* and previous measurements of LPA receptor distribution.

Vzg-1 and LPA Signaling Have Potential Functions in Cortical Neurogenesis

In situ hybridization and BrdU double labeling experiments demonstrate that *vzg-1* is expressed within the embryonic vz and is both temporally and spatially related to the period of cortical neurogenesis (67, 68) (Figs. 1 *b* and 5). The identification of the *vzg-1* gene product as a receptor for LPA suggests that LPA signaling mechanisms may be important in regulating cortical neurogenesis. Possible

Table IV. Vzg-1 Sense Overexpression Increases the Potency of LPA to Induce Cell Rounding and Inhibit Adenylate Cyclase

| Cell Line | Cell rounding | | | | Adenylate cyclase inhibition | |
	EC₅₀ (nM) (95% confidence interval)	−logEC₅₀ ± SEM	Minimum response (Percent round, mean ± SEM)	Maximum response (Percent round, mean ± SEM)	EC₅₀ (nM) (95% confidence interval)	−logEC₅₀ ± SEM
Sense (line 3)	1.3 (0.74–2.3)	8.89 ± 0.12	38 ± 2.1	75 ± 1.2	5.9 (3.0–12)	8.23 ± 0.15
Antisense (line 17)	10 (5.9–18)	7.98 ± 0.12	22 ± 1.4	54 ± 1.3	34 (13–89)	7.47 ± 0.21
Control (line 33)	9.0 (5.0–17)	8.04 ± 0.13	35 ± 1.9	77 ± 1.8	39 (13–113)	7.41 ± 0.23

Cells were serum deprived for 24 h and then stimulated for 15 min with LPA for cell rounding or for 7 min for cyclase inhibition. Cell rounding values were calculated from data obtained from three independent experiments, each done in duplicate (c.f. Fig. 7 *c*). Cyclase inhibition values were calculated from data obtained from four independent concentration-response experiments, each done in triplicate (data not shown).
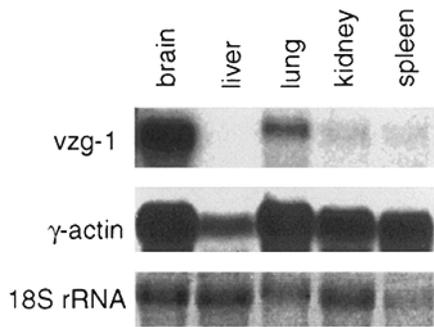
Figure 8. Tissue expression of *vzg-1* parallels previous estimates of LPA receptor tissue distribution. *Vzg-1* Northern blot analysis (10 µg total RNA) of adult tissue demonstrates that *vzg-1* is highly expressed in the adult brain, absent from liver, and present in moderate levels in lung, kidney, and spleen, which correlates strongly with previous estimates of LPA receptor distribution (71, 77). Variable expression of the γ-actin loading control (cf. Fig. 3) reflects documented differences in expression amongst tissues (28), necessitating use of the 18S rRNA band, visualized with ethidium bromide.

functions of LPA in cortical neurogenesis, based on known bioactivities of LPA and biological events occurring within the vz, include regulation of cytoskeletal events such as interkinetic nuclear movement, cell rounding, and cleavage plane orientation (13, 40), mitogenesis (discussed below), gap junction regulation (34, 49), and influence on the binding and assembly of fibronectin (11, 83), which is expressed in the embryonic cortex (15, 65). Additionally, regulation of apoptosis, recently shown to occur in the vz (5), may also be influenced by LPA signaling (47). The actual roles of LPA signaling in the vz, mediated through *vzg-1*, and the source of endogenous ligand remain to be determined.

Vzg-1 Expression Implicates Distinct GPCR-mediated Signaling Pathways in Cortical Neurogenesis

The major signal transduction elements currently implicated in cortical neurogenesis operate through peptide ligand stimulation of the RTK pathway (70). By contrast, the bioactive lipid LPA operates through Vzg-1, a GPCR family member. Prior studies on LPA signaling have demonstrated that LPA activates heterotrimeric G proteins, as well as small GTPases such as Rho that are positioned downstream in the signaling pathway (54). Therefore, many of the initial signaling steps mediated by LPA are distinct from the RTK pathway. The presence of *vzg-1* expression within the cerebral cortical vz indicates the existence of a specific role for heterotrimeric G protein signaling in cortical neurogenesis.

In view of *vzg-1* expression in the zone of neuroblast proliferation, there is a possible role for mitogenic signaling mediated by LPA in cortical neuron generation. Mitogenic effects of LPA appear to involve activation of two signaling pathways. The PTX-sensitive pathway, involving activation of G_i and Ras (74, 76), is probably mediated through βγ subunit signaling (21, 50, 51). The PTX-insensitive pathway depends on functional Rho and might lead to cell proliferation through activation of a mitogen-activated protein kinase cascade (33, 35). Functional Rho is

also necessary for actin-based cytoskeletal changes (40, 61). Our results directly demonstrate the activation of the PTX-sensitive G_i-linked pathway, and indirectly demonstrate the activation of the PTX-insensitive pathway leading to Rho activation, by *vzg-1* mediated LPA signaling in neocortical neuroblast cell lines. Thus, a single LPA receptor appears to mediate distinct signaling pathways. The possible interactions between RTK pathways and these G protein mediated events during cortical development will be addressed in future studies. Understanding these and related factors controlling cortical neurogenesis may provide new insights into the observed increase in cerebral cortical size with phylogenetic ascension.

In addition to roles in neural development, this LPA receptor may participate in the functioning of many other developing and adult tissues and cell types, based on the diversity of effects known to be stimulated by LPA. Availability of a cDNA encoding a receptor for LPA should facilitate the molecular genetic characterization of LPA receptor–dependent interactions in various cell and tissue types and allow the development of agents that can be used to manipulate LPA receptor signaling pathways. The physiological consequences of LPA receptor elimination in mice, the sites of LPA production in vivo, and the possible role of this receptor in pathological states remain to be determined.

References

1. Allen, L., R. Lefkowitz, M. Caron, and S. Cotecchia. 1991. G protein-coupled receptor genes as protooncogenes: constitutively activating mutation of the α1B-adrenergic receptor enhances mitogenesis and tumorigenicity. *Proc. Nat. Acad. Sci. USA.* 88:11354–11358.
2. Ausubel, F.M., R. Brent, R.E. Kingston, D.D. Moore, J.G. Seidman, J.A. Smith, and K. Struhl. 1994. Current Protocols in Molecular Biology. John Wiley & Sons, Inc., New York.
3. Barbacid, M. 1995. Neurotrophic factors and their receptors. *Curr. Opin. Cell Biol.* 7:148–155.
4. Berry, M., and A.W. Rogers. 1965. The migration of neuroblasts in the developing cerebral cortex. *J. Anat.* 99:691–709.
5. Blaschke, A.J., K. Staley, and J. Chun. 1996. Widespread programmed cell death in proliferative and postmitotic regions of the fetal cerebral cortex. *Development (Camb.).* 122:1165–1174.
6. Boulder Committee. 1970. Embryonic vertebrate central nervous system: revised terminology. *Anat. Rec.* 166:257–261.
7. Buck, L., and R. Axel. 1991. A novel multigene family may encode odorant receptors: a molecular basis for odor recognition. *Cell.* 65:175–187.
8. Cattneo, E., and R. McKay. 1990. Proliferation and differentiation of neuronal stem cells regulated by nerve growth factor. *Nature (Lond.).* 347: 762–765.
9. Caviness, V.S., Jr. 1973. Time of neuron origin in the hippocampus and dentate gyrus of normal and reeler mutant mice: an autoradiographic analysis. *J. Comp. Neurol.* 151:113–120.
10. Caviness, V.S., Jr. 1982. Neocortical histogenesis in normal and reeler mice: a developmental study based upon ³H-thymidine autoradiography. *Dev. Brain Res.* 4:293–302.
11. Checovich, W.J., and D.F. Mosher. 1993. Lysophosphatidic acid enhances

fibronectin binding to adherent cells. *Arterioscler. Thromb.* 13:1662–1667.

12. Chen, C., and H. Okayama. 1987. High-efficiency transformation of mammalian cells by plasmid DNA. *Mol. Cell. Biol.* 7:2745–2752.

13. Chenn, A., and S.K. McConnell. 1995. Cleavage orientation and the asymmetric inheritance of Notch1 immunoreactivity in mammalian neurogenesis. *Cell.* 82:631–641.

14. Chun, J., and R. Jaenisch. 1996. Clonal cell lines produced by infection of neocortical neuroblasts using multiple oncogenes transduced by retroviruses. *Mol. Cell. Neurosci.* 7:304–321.

15. Chun, J.J.M., and C.J. Shatz. 1988. A fibronectin-like molecule is present in the developing cat cerebral cortex and is correlated with subplate neurons. *J. Cell Biol.* 106:857–872.

16. Chun, J.J.M., and C.J. Shatz. 1988. Redistribution of synaptic vesicle antigens is correlated with the disappearance of a transient synaptic zone in the developing cerebral cortex. *Neuron.* 1:297–310.

17. Chun, J.J.M., and C.J. Shatz. 1989. Interstitial cells of the adult neocortical white matter are the remnant of the early generated subplate neuron population. *J. Comp. Neurol.* 282:555–569.

18. Chun, J.J.M., and C.J. Shatz. 1989. The earliest-generated neurons of the cat cerebral cortex: characterization by MAP2 and neurotransmitter immunohistochemistry during fetal life. *J. Neurosci.* 9:1648–1677.

19. Chun, J.J.M., D.G. Schatz, M.A. Oettinger, R. Jaenisch, and D. Baltimore. 1991. The recombination activating gene-1 (RAG-1) transcript is present in the murine central nervous system. *Cell.* 64:189–200.

20. Cooper, J.R., F.E. Bloom, and R.H. Roth. 1991. The Biochemical Basis of Neuropharmacology. Oxford University Press, Oxford. 454 pp.

21. Crespo, P., N. Xu, W.F. Simonds, and J.S. Gutkind. 1994. Ras-dependent activation of MAP kinase pathway mediated by G protein $\beta\gamma$ subunits. *Nature (Lond.).* 369:418–420.

22. Das, G.D. 1979. Gliogenesis and ependymogenesis during embryonic development of the rat. An autoradiographic study. *J. Neurol. Sci.* 43:193–204.

23. Desarnaud, F., O. Labbe, D. Eggerickx, G. Vassart, and M. Parmentier. 1994. Molecular cloning, functional expression and pharmacological characterization of a mouse melanocortin receptor gene. *Biochem. J.* 299:367–373.

24. Dohlman, H.G., M. Bouvier, J.L. Benovic, M.G. Caron, and R.J. Lefkowitz. 1987. The multiple membrane spanning topography of the β2-adrenergic receptor. Localization of the sites of binding, glycosylation, and regulatory phosphorylation by limited proteolysis. *J. Biol. Chem.* 262:14282–14288.

25. Donnelly, J.J., D. Martinez, K.U. Jansen, R.W. Ellis, D.L. Montgomery, and M.A. Liu. 1996. Protection against papillomavirus with a polynucleotide vaccine. *J. Infect. Dis.* 173:314–320.

26. Durieux, M.E. 1995. Lysophosphatidate Signaling: Cellular Effects and Molecular Mechanisms. R.G. Landes Company, Austin, TX. 241 pp.

27. Eichholtz, T., K. Jalink, I. Fahrenfort, and W.H. Moolenaar. 1993. The bioactive phospholipid lysophosphatidic acid is released from activated platelets. *Biochem. J.* 291:677–680.

28. Erba, H.P., R. Eddy, T. Shows, L. Kedes, and P. Gunning. 1988. Structure, chromosome location, and expression of the human γ-actin gene: differential evolution, location, and expression of the cytoskeletal β- and γ-actin genes. *Mol. Cell. Biol.* 8:1775–1789.

29. Fourcade, O., M.F. Simon, C. Viode, N. Rugani, F. Leballe, A. Ragab, B. Fournie, L. Sarda, and H. Chap. 1995. Secretory phospholipase A2 generates the novel lipid mediator lysophosphatidic acid in membrane microvesicles shed from activated cells. *Cell.* 80:919–927.

30. Ghosh, A., and M.E. Greenberg. 1995. Distinct roles for bFGF and NT-3 in the regulation of cortical neurogenesis. *Neuron.* 15:89–103.

31. Hausdorff, W.P., M.G. Caron, and R.J. Lefkowitz. 1990. Turning off the signal: desensitization of β-adrenergic receptor function. *FASEB J.* 4:2881–2889.

32. Hicks, S.P., and C.J. D'Amato. 1968. Cell migrations to the isocortex in the rat. *Anat. Rec.* 160:619–634.

33. Hill, C.S., and R. Treisman. 1995. Differential activation of c-fos promoter elements by serum, lysophosphatidic acid, G proteins and polypeptide growth factors. *EMBO (Eur. Mol. Biol. Organ.) J.* 14:5037–5047.

34. Hill, C.S., S.Y. Oh, S.A. Schmidt, K.J. Clark, and A.W. Murray. 1994. Lysophosphatidic acid inhibits gap-junctional communication and stimulates phosphorylation of connexin-43 in WB cells: possible involvement of the mitogen-activated protein kinase cascade. *Biochem. J.* 303:475–479.

35. Hill, C.S., J. Wynne, and R. Treisman. 1995. The Rho family GTPases RhoA, Rac1, and CDC42Hs regulate transcriptional activation by SRF. *Cell.* 81:1159–1170.

36. Hla, T., and T. Maciag. 1990. An abundant transcript induced in differentiating human endothelial cells encodes a polypeptide with structural similarities to G protein-coupled receptors. *J. Biol. Chem.* 265:9308–9313.

37. Ishii, K., L. Hein, B. Kobilka, and S.R. Coughlin. 1993. Kinetics of thrombin receptor cleavage on intact cells. Relation to signaling. *J. Biol. Chem.* 268:9780–9786.

38. Jalink, K., and W.H. Moolenaar. 1992. Thrombin receptor activation causes rapid neural cell rounding and neurite retraction independent of classic second messengers. *J. Cell Biol.* 118:411–419.

39. Jalink, K., T. Eichholtz, F.R. Postma, E.J. van Corven, and W.H.

Moolenaar. 1993. Lysophosphatidic acid induces neuronal shape changes via a novel, receptor-mediated signaling pathway: similarity to thrombin action. *Cell Growth Differ.* 4:247–255.

40. Jalink, K., E.J. van Corven, T. Hengeveld, N. Morii, S. Narumiya, and W.H. Moolenaar. 1994. Inhibition of lysophosphatidate- and thrombin-induced neurite retraction and neuronal cell rounding by ADP ribosylation of the small GTP-binding protein Rho. *J. Cell Biol.* 126:801–810.

41. Julius, D., T. Livelli, T. Jessell, and R. Axel. 1989. Ectopic expression of the serotonin 1c receptor and the triggering of malignant transformation. *Science (Wash. DC).* 244:1057–1062.

42. Karnik, S.S., and H.G. Khorana. 1990. Assembly of functional rhodopsin requires a disulfide bond between cysteine residues 110 and 187. *J. Biol. Chem.* 265:17520–17524.

43. Kilpatrick, T.J., and P.F. Bartlett. 1993. Cloning and growth of multipotential neural precursors: requirements for proliferation and differentiation. *Neuron.* 10:255–265.

44. Kilpatrick, T.J., and P.F. Bartlett. 1995. Cloned multipotential precursors from the mouse cerebrum require FGF-2, whereas glial restricted precursors are stimulated with either FGF-2 or EGF. *J. Neurosci.* 15:3653–3661.

45. Klein, R. 1994. Role of neurotrophins in mouse neuronal development. *FASEB J.* 8:738–744.

46. Kyte, J., and R.F. Doolittle. 1982. A simple method for displaying the hydropathic character of a protein. *J. Mol. Biol.* 157:105–132.

47. Lauener, R., Y. Shen, V. Duronio, and H. Salari. 1995. Selective inhibition of phosphatidylinositol 3-kinase by phosphatidic acid and related lipids. *Biochem. Biophys. Res. Comm.* 215:8–14.

48. Libert, F., M. Parmentier, A. Lefort, C. Dinsart, J. Van Sande, C. Maenhaut, M. Simons, J. Dumont, and G. Vassart. 1989. Selective amplification and cloning of four new members of the G protein-coupled receptor family. *Science (Wash. DC).* 244:569–572.

49. Lo Turco, J.J., and A.R. Kriegstein. 1991. Clusters of coupled neuroblasts in embryonic neocortex. *Science (Wash. DC).* 252:563–566.

50. Luttrell, L.M., B.E. Hawes, K. Touhara, T. van Biesen, W.J. Koch, and R.J. Lefkowitz. 1995. Effect of cellular expression of pleckstrin homology domains on G_i-coupled receptor signaling. *J. Biol. Chem.* 270:12984–12989.

51. Luttrell, L.M., T. van Biesen, B.E. Hawes, W.J. Koch, K. Touhara, and R.J. Lefkowitz. 1995. G $\beta\gamma$ subunits mediate mitogen-activated protein kinase activation by the tyrosine kinase insulin-like growth factor 1 receptor. *J. Biol. Chem.* 270:16495–16498.

52. Matsuda, L.A., S.J. Lolait, M.J. Brownstein, A.C. Young, and T.I. Bonner. 1990. Structure of a cannabinoid receptor and functional expression of the cloned cDNA. *Nature (Lond.).* 346:561–564.

53. Mead, D.A., N.K. Pey, C. Herrnstadt, R.A. Marcil, and L.M. Smith. 1991. A universal method for the direct cloning of PCR amplified nucleic acid. *Biotechnology.* 9:657–663.

54. Moolenaar, W.H. 1995. Lysophosphatidic acid signalling. *Curr. Opin. Cell Biol.* 7:203–210.

55. Post, S.R., J.P. Jacobson, and P.A. Insel. 1996. P2 purinergic receptor agonists enhance cAMP production in Madin-Darby canine kidney epithelial cells via an autocrine/paracrine mechanism. *J. Biol. Chem.* 271:2029–2032.

56. Pratt, W.B., and P. Taylor. 1990. Principles of Drug Action: The Basis of Pharmacology. Churchill Livingstone, New York. 836 pp.

57. Probst, W.C., L.A. Snyder, D.I. Schuster, J. Brosius, and S.C. Sealfon. 1992. Sequence alignment of the G protein coupled receptor superfamily. *DNA Cell Biol.* 11:1–20.

58. Rakic, P. 1988. Specification of cerebral cortical areas. *Science (Wash. DC).* 241:170–176.

59. Rands, E., M.R. Candelore, A.H. Cheung, W.S. Hill, C.D. Strader, and R.A. Dixon. 1990. Mutational analysis of β-adrenergic receptor glycosylation. *J. Biol. Chem.* 265:10759–10764.

60. Raz, E., D.A. Carson, S.E. Parker, T.B. Parr, A.M. Abai, G. Aichinger, S.H. Gromkowski, M. Singh, D. Lew, M.A. Yankauckas, et al. 1994. Intradermal gene immunization: the possible role of DNA uptake in the induction of cellular immunity to viruses. *Proc. Natl. Acad. Sci. USA.* 91:9519–9523.

61. Ridley, A.J., and A. Hall. 1992. The small GTP-binding protein Rho regulates the assembly of focal adhesions and actin stress fibers in response to growth factors. *Cell.* 70:389–399.

62. Sauer, F.C. 1935. Mitosis in the neural tube. *J. Comp. Neurol.* 62:377–405.

63. Seymour, R.M., and M. Berry. 1975. Scanning and transmission electron microscope studies of interkinetic nuclear migration in the cerebral vesicles of the rat. *J. Comp. Neurol.* 160:105–125.

64. Sidman, R., I. Miale, and N. Feder. 1959. Cell proliferation and migration in the primitive ependymal zone: an autoradiographic study of histogenesis in the nervous system. *Exp. Neurol.* 1:322–333.

65. Stewart, G.R., and A.L. Pearlman. 1987. Fibronectin-like immunoreactivity in the developing cerebral cortex. *J. Neurosci.* 7:3325–3333.

66. Suidan, H.S., S.R. Stone, B.A. Hemmings, and D. Monard. 1992. Thrombin causes neurite retraction in neuronal cells through activation of cell surface receptors. *Neuron.* 8:363–375.

67. Takahashi, T., R.S. Nowakowski, and V.S. Caviness Jr. 1993. Cell cycle parameters and patterns of nuclear movement in the neocortical proliferative zone of the fetal mouse. *J. Neurosci.* 13:820–833.

68. Takahashi, T., R.S. Nowakowski, and V.S. Caviness Jr. 1995. The cell cycle

of the pseudostratified ventricular epithelium of the embryonic murine cerebral wall. *J. Neurosci.* 15:6046–6057.

69. Temple, S., and A.A. Davis. 1994. Isolated rat cortical progenitor cells are maintained in division in vitro by membrane-associated factors. *Development (Camb.).* 120:999–1008.

70. Temple, S., and X. Qian. 1995. bFGF, neurotrophins, and the control of cortical neurogenesis. *Neuron.* 15:249–252.

71. Thomson, F.J., L. Perkins, D. Ahern, and M. Clark. 1994. Identification and characterization of a lysophosphatidic acid receptor. *Mol. Pharmacol.* 45:718–723.

72. Tokumura, A., M. Iimori, Y. Nishioka, M. Kitahara, M. Sakashita, and S. Tanaka. 1994. Lysophosphatidic acids induce proliferation of cultured vascular smooth muscle cells from rat aorta. *Am. J. Physiol.* 267:C204–C210.

73. Turka, L.A., D.G. Shatz, M.A. Oettinger, J.J.M. Chun, C. Gorka, K. Lee, W.T. McCormack, and C.B. Thompson. 1991. Thymocyte expression of the recombination activating genes RAG-1 and RAG-2 can be terminated by T-cell receptor stimulation in vitro. *Science (Wash. DC).* 253:778–781.

74. van Corven, E.J., A. Groenink, K. Jalink, T. Eichholtz, and W.H. Moolenaar. 1989. Lysophosphatidate-induced cell proliferation: identification and dissection of signaling pathways mediated by G proteins. *Cell.* 59:45–54.

75. van Corven, E.J., A. van Rijswijk, K. Jalink, R.L. van der Bend, W.J. van Blitterswijk, and W.H. Moolenaar. 1992. Mitogenic action of lysophosphatidic acid and phosphatidic acid on fibroblasts. Dependence on acyl-chain length and inhibition by suramin. *Biochem. J.* 281:163–169.

76. van Corven, E.J., P.L. Hordijk, R.H. Medema, J.L. Bos, and W.H. Moolenaar. 1993. Pertussis toxin-sensitive activation of p21ras by G protein-coupled receptor agonists in fibroblasts. *Proc. Natl. Acad. Sci. USA.* 90:1257–1261.

77. van der Bend, R.L., J. Brunner, K. Jalink, E.J. van Corven, W.H. Moolenaar, and W.J. van Blitterswijk. 1992. Identification of a putative membrane receptor for the bioactive phospholipid, lysophosphatidic acid. *EMBO (Eur. Mol. Biol. Organ.) J.* 11:2495–2501.

78. van der Geer, P., T. Hunter, and R.A. Lindberg. 1994. Receptor protein-tyrosine kinases and their signal transduction pathways. *Annu. Rev. Cell Biol.* 10:251–337.

79. Vara, J.A., A. Portela, J. Ortin, and A. Jimenez. 1986. Expression in mammalian cells of a gene from Streptomyces alboniger conferring puromycin resistance. *Nucleic Acids Res.* 14:4617–4624.

80. Watson, S., and S. Arkinstall. 1994. The G-Protein Linked Receptor Factsbook. Academic Press, London. 427 pp.

81. Xu, Y., G. Casey, and G.B. Mills. 1995. Effect of lysophospholipids on signaling in the human Jurkat T cell line. *J. Cell Physiol.* 163:441–450.

82. Yoshida, S., A. Fujisawasehara, T. Taki, K. Arai, and Y. Nabeshima. 1996. Lysophosphatidic acid and bFGF control different modes in proliferating myoblasts. *J. Cell Biol.* 132:181–193.

83. Zhang, Q., W.J. Checovich, D.M. Peters, R.M. Albrecht, and D.F. Mosher. 1994. Modulation of cell surface fibronectin assembly sites by lysophosphatidic acid. *J. Cell Biol.* 127:1447–1459.